3. HYDROGEOLOGIC SETTING OF THE PROPOSED SITE

This section describes INTEC hydrogeologic and physical characteristics to establish a framework on which to base site screening. Topics summarized include geology, site specific physiography, soils, surface and subsurface hydrology, meteorology and climatology, groundwater protection and quality, flora and fauna, archeological resources, demography and land use, and infrastructure.

3.1 Geology

3.1.1 Regional Geologic Setting

The INTEC is situated on the Eastern Snake River Plain (ESRP) in southeast Idaho—a low-relief, low-elevation basin flanked by high mountains of the Northern Rocky Mountains and the northern Basin and Range Province. The ESRP, an elongated basin extending from the Yellowstone Plateau on the northeast to the Twin Falls area on the southwest, is floored by basalt lava flows and various sediments of alluvial, eolian, and lacustrine origin. It is a volcanic province that formed in response to movement of the North American tectonic plate southwestwardly across the Yellowstone hot spot. Explosive rhyolitic volcanic eruptions produced extensive deposits of rhyolitic pyroclastic deposits in the ESRP between 10 and 4 million years ago. The ESRP has been subsiding and filling with basaltic lava flows and sediments for the past 4 million years. Large basin-and-range normal faults adjacent to the ESRP and basaltic volcanism on the ESRP are ongoing geologic processes that generate seismic and volcanic hazards for INEEL facilities. A detailed summary of the regional geologic history is given by Hackett and Smith (1992).

3.1.2 INTEC Area and Site Specific Physiography and Geology

The INTEC and the proposed location of new ponds are located in a flat-lying area just southeast of the Big Lost River channel in the south-central part of the INEEL. In this area, alluvial gravels from the Big Lost River cover a broad area that is about 6 km (3.7 mi) wide, bounded on the southeast and northwest by outcrops of basalt lava flows. The INTEC is sited on Late Pleistocene alluvial gravels on a low terrace above the Holocene floodplain. The Holocene floodplain, which lies between the INTEC and the TRA, is characterized by numerous abandoned channels and possibly braided channels of the Big Lost River. The presently active channel, which has been dry at INTEC approximately 4 of the last 10 years, is incised into the Holocene floodplain deposits by about 1.5 to 2 m (4.9 to 6.5 ft), and is floored by light tan color sands and fine gravels. Air photographs of the pleistocene terrace deposit on which the INTEC is located shows no evidence of recent channels or braids of the river. A subdued meander-scroll topography is present over large areas of the Pleistocene surface, especially to the south and southwest of INTEC (Figure 3-1). The surface is covered by sagebrush and the meander-scrolls are recognizable mainly from tonal anomalies on air photographs. Based on the degree of soil development and radiocarbon ages of sediments, the deposits that make up this surface were laid down during periods of high runoff during retreat of the most recent (Pinedale) glaciers, probably in the range of 15,000 to 20,000 years ago (Scott 1982, Ostenaa et al. 1999).

The landforms adjacent to the Big Lost River alluvial deposits are dominated by lava flow surface morphology that has been subdued somewhat by deposition of loess and fine eolian sand in low areas and in the lees of ridges and hills (Figure 3-2). The lava flow surfaces are characterized by rugged but low-relief topography. Due to deflation of parts of the surface during waning stages of volcanic activity, there are numerous closed basins separated by undeflated ridges. The largest of the basins (up to several tens of meters across) commonly contain thin playa deposits which cover the basin floors. The ridges are riddled with anastomosing fissures that are roughly parallel to the margins of the collapsed basins. Many of the outcrops show columnar jointing that produces a hexagonal or polygonal pattern of fractures on the outcrop surface.

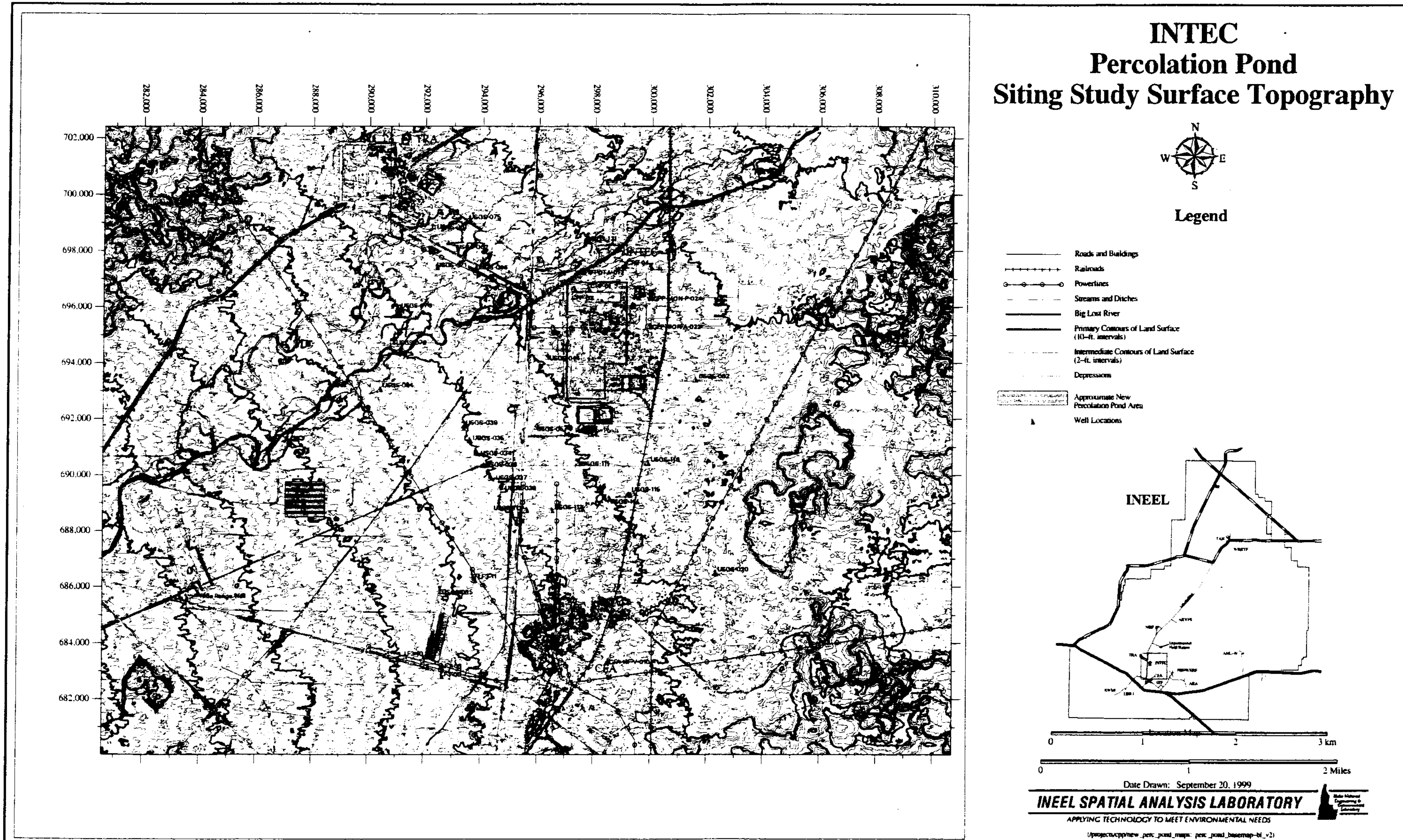

Figure 3-1. Surface topography of the INTEC and surrounding area.

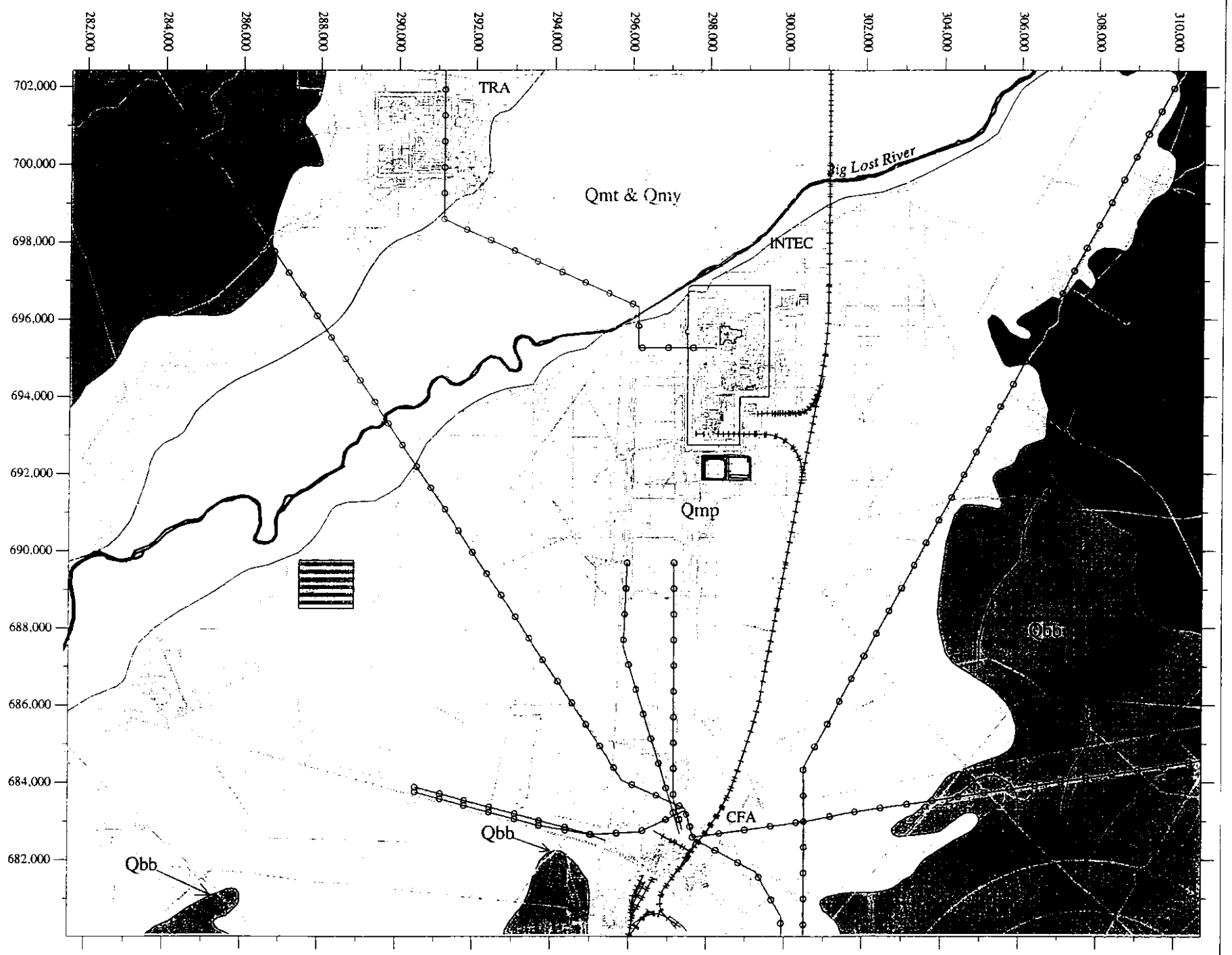

Geologic Map of the INTEC/CFA Area

N
W E
S

Legend

- Roads and Buildings
- Railroads
- Powerlines
- Existing Percolation Ponds, Tank Farm, INTEC Boundary
- Big Lost River
- Approximate New Percolation Pond Area
- Qmy – Modern Flood Plains. Alluvial deposits of sand, pebble gravel, silt, and clay; locally humic in poorly drained areas. Subject to flooding.
- Qmt – Holocene to Upper Pleistocene Alluvial deposits. Pebble and cobble gravel to pebbly sand; minor silty sand.
- Qmp – Pinedale Alluvial deposits along main streams. Pebble and cobble gravel to pebbly sand; minor sand. Upper 0.5–2m generally includes a mixed sand and silt of eolion origin and/or alluvial origin. Forms terraces along Big Lost River.
- Qbb – Basaltic lava flows of ~15–200 ka age (upper to middle Pleistocene). Dark gray to black pahoehoe flows. Locally covered by up to 1m of eolian sand and loess. Normal magnetic polarization. Flowed from Butte 5206, just north of Big Southern Butte.
- Qbc – Basaltic lava flow of middle Pleistocene age. Age = 230 ka. Dark gray pahoehoe. Locally covered by several meters of eolian sand and loess. Normal magnetic polarity. Flowed from Mid Butte.
- Qbd – Basaltic lava flow of middle to lower pleistocene age. Age = 520 ka. Dark gray pahoehoe. Locally covered by several meters of eolian sand and loess. Normal magnetic polarity. Flowed from vent at Creater Peak.
- Well Locations

0 1 2 3 km

0 1 2 Miles

Date Drawn: September 20, 1999

INEEL SPATIAL ANALYSIS LABORATORY

APPLYING TECHNOLOGY TO MEET ENVIRONMENTAL NEEDS

(/projects/cpp/new_perc_pond_maps: geology_and_base-bl_v1)

Figure 3-2. Geologic map of the INTEC and CFA areas.

The basalts at the surface just east of INTEC (Figure 3-2), and perhaps lying beneath the surficial sediment layer, are about 230,000 years old and flowed from vents located about 14 km (8.6 mi) southeast of the site (Kuntz et al. 1994). Basalt flows beneath those at the surface are older—as much as about 4.3 million years old at the base of the basalt sequence (Hackett and Smith 1992). These basalts have accumulated in the ESRP basin that has continuously subsided at a rate of about 0.5 mm/year since passage of the Yellowstone hot spot about 4.3 million years ago (Pierce and Morgan 1992).

Basalts in the INTEC area, and throughout most of the ESRP, are olivine tholeiites. They are mostly porphyritic and contain up to 20% by volume phenocrysts of olivine and plagioclase. The groundmass is composed of olivine, plagioclase, clinopyroxene, magnetite, ilmenite, and minor amounts of apatite, glass, rutile, and oxidation products. An average of 78 chemical analyses and ion exchange capacity on a fresh sample of basalt from the subsurface at INEEL can be found in Leeman 1982 and Nace et al. 1975, respectively.

3.1.3 Stratigraphy

At INTEC, the surficial sediments (Big Lost River alluvium) vary from 9 to 18 m (30 to 60 ft) thick and consist mostly of gravel, gravelly sands, and sands deposited by the Big Lost River during late Pleistocene time. In some locations, a thin (0 to 2 m [0 to 6 ft] thick) layer of clay and silt underlies the gravelly alluvium, forming a discontinuous low-permeability layer just above the basalt bedrock (Golder Associates 1992). The surficial sediments overlie an alternating sequence of basalt lava flows and interbedded sediments known as the Snake River Group, extending to a depth of 600 to 700 m (1,968 to 2,296 ft). Basalt lava flow groups make up at least 85% of the upper 213 m (700 ft) of stratigraphy beneath INTEC, the remainder being sediment interbeds.

Although the surficial sediment at INTEC is composed of alluvial gravels, sedimentary interbeds within the Snake River Group are composed mostly of silts, clayey silts, and sandy silts of both alluvial and eolian origin. Some of the deeper, thicker interbeds contain significant alluvial materials, including sands and gravels, and, at the northern end of the INTEC near the course of the Big Lost River, some of the interbeds within the vadose zone contain sands and gravels. A cross section showing the positions and thickness of interbeds is presented in Figure 3-3 (based on Anderson 1991). This section shows that the first major interbed occurs at a depth of about 45 to 60 m (148 to 197 ft) below the surface. Several more interbeds occur between 60 and 180 m (197 to 591 ft), and throughout the entire thickness of the basalt section (between 0.7 and 1.1 km [0.43 and 0.68 mi] in this area) because they are present in deep exploration wells INEEL-1 (Figure 3-4), located about 5 km (3.1 mi) north of INTEC, and WO-2, located about 5 km (3.1 mi) to the east.

Stratigraphic interpretations in the WAG 3 conceptual model required that various stratigraphic units be combined for simplification. The shallow interbed (approximately 34 m [110 ft] bls) and the deep interbed (approximately 116 m [380 ft] bls) are assumed to be the primary perching layers beneath the INTEC and are assumed to be continuous. In reality, however, the stratigraphy is highly complex and poorly understood.

Based on analyses of geophysical logs of wells, examination of drill core from coreholes, chemical analyses of core samples, and radiometric age determinations, 23 basalt lava-flow groups have been identified in the first 213 m (700 ft) beneath INTEC (Anderson 1991). These flow groups have been "named" with the letter designations shown in Figure 3-3. Because the detailed stratigraphic work was initiated at the RWMC (Anderson and Lewis 1989), about 9 km (5.6 mi) south of INTEC, the "named" groups there have been extended to correlative units beneath the INTEC area. Additional groups have been identified beneath the INTEC area and thus letter

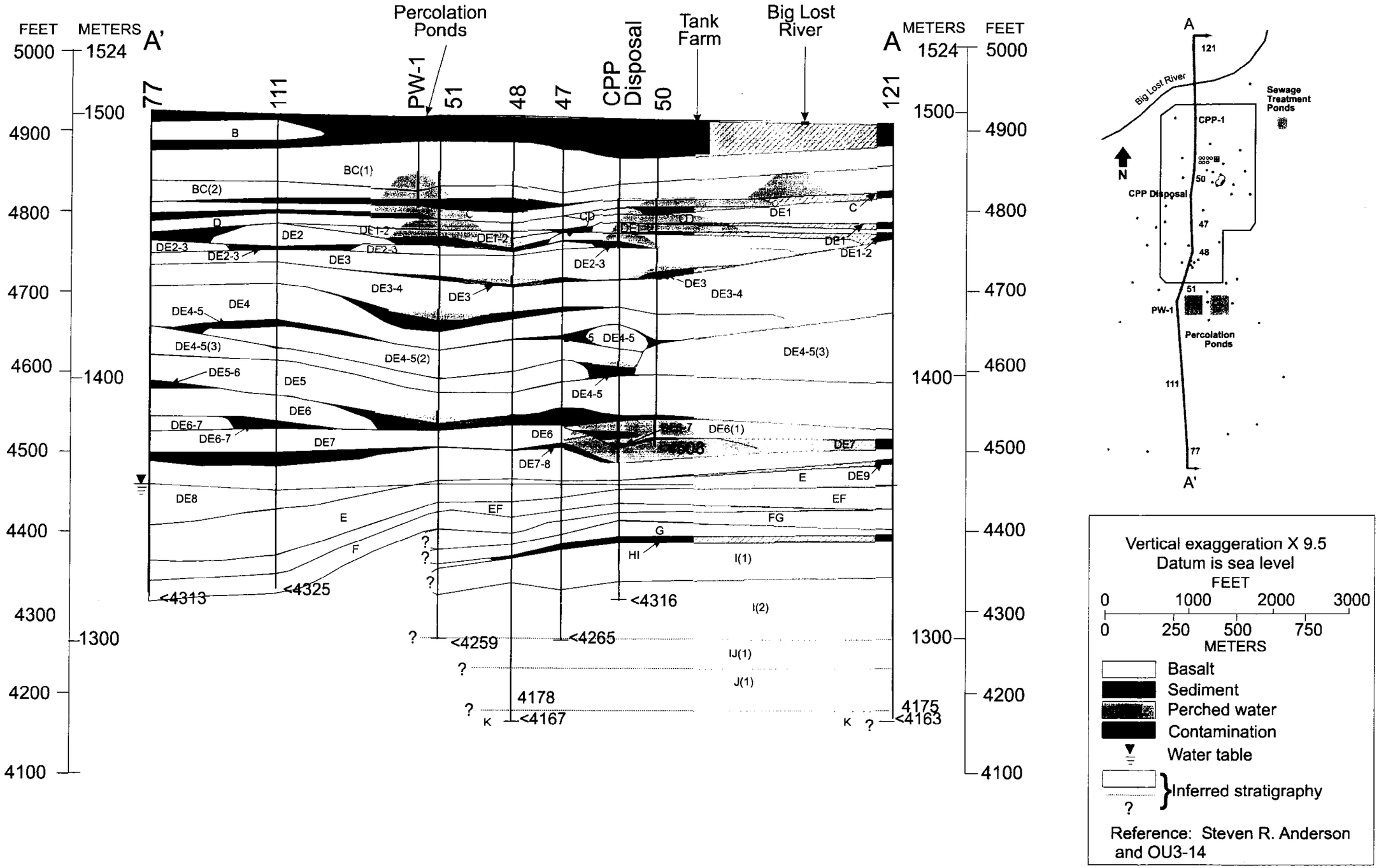

Figure 3-3. Stratigraphic cross-section through INTEC

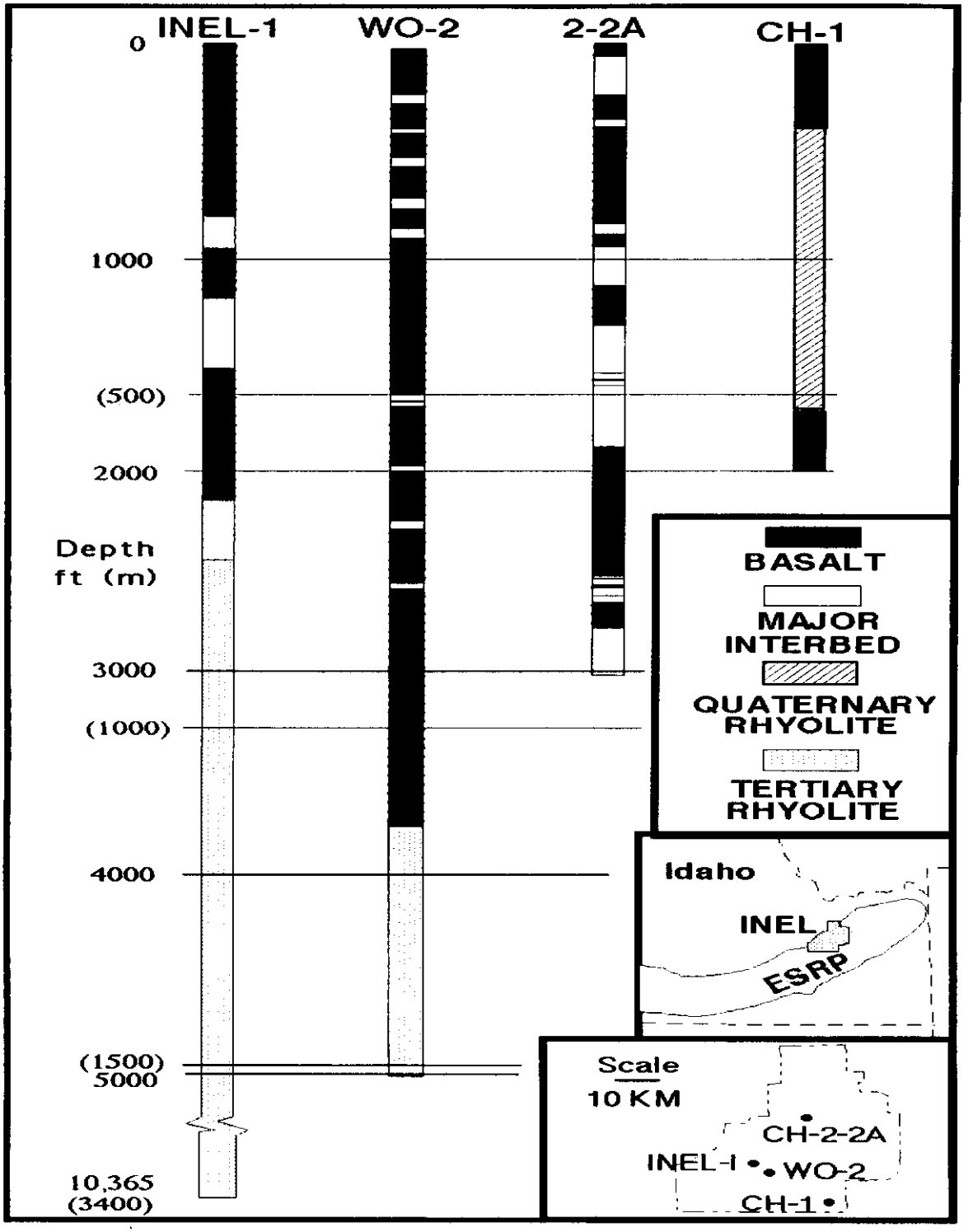

Simplified lithologic logs of deep drillholes on the INEL.
(INEL-1 from Doherty et al., 1979; CH-1 from Doherty, 1979a;
2-2A from Doherty, 1979b; and WO-2 from Hackett and Smith, 1992)

Figure 3-4. Simplified lithologic logs of four deep INEEL drill holes.

designations such as DE-1, DE-2, have been developed. In general, Flow Group B is the youngest recognized at INTEC and Flow Group I is the oldest. The age of Flow Group B is about 100,000 years and the age of Flow Group I is about 640,000 years.

Flow Group I erupted from AEC Butte, which lies less than 2 km (1.2 mi) north of TRA, and covers a large portion of southern INEEL. It has a distinctive chemistry and petrography that allows for easy identification in geophysical logs (gamma logs) and drill core. Flow group F is easily recognized by its paleomagnetic properties because it was emplaced during a short period of reversed magnetic polarity about 565,000 years ago (Champion et al. 1988). It probably flowed into the INTEC area from a vent to the southwest, somewhere in the Arco Volcanic Rift Zone.

The thickness of surficial sediment at INTEC (8 to >15 m [26 to >49 ft]) is greater than that of most interbeds in the vadose zone beneath the site. Down to about 122 m (400 ft), interbeds in the vadose zone range from 1 to 4.7 m (3.2 to 15.4 ft) thick, with an average of about 2.6 m (8.5 ft) thick. At greater depths in the sequence, interbeds are even thicker (see Figure 3-4). At depths of about 500 m (1,600 ft) and greater, several interbeds occur that are 10 to 30 m (30 to 100 ft) thick, with an average thickness of about 8.4 m (28 ft) from 500 m (1,640 ft) to the base of the basalt-sediment sequence. On an INEEL-wide basis, the thickness of sediment interbed distributions are similar to that beneath INTEC. For all INEEL wells and drill holes, interbeds tend to be thinner at depths less than 305 m (1,000 ft) (mean =17 ft; median = 9 ft) and thicker at depths greater than 305 m (1,000 ft) (mean = 38 ft; median = 25 ft). In addition, the thickness of interbeds tends to be greater in the northern part of INEEL (median ~ 4.9 m [16 ft]) than in the southern and southeastern parts (median ~ 2.1 m [7 ft]).

Site-specific stratigraphy for the proposed location of the new facility is not characterized. The closest stratigraphic information is found in USGS-84, USGS-85, the Rifle Range Well, and the arc of wells southwest of INTEC. Cross-sections by Anderson 1991 (Figures 3-5 and 3-6), present stratigraphic interpretations which may or may not be representative of the proposed site. Efforts associated with the wastewater land application permitting process will require the installation of four new aquifer wells around the new facility. Information from these wells will be used to characterize the subsurface within the immediate vicinity of the new percolation ponds.

3.1.4 Seismic Hazards

Ground shaking, caused by earthquakes on the basin and range normal faults north of the ESRP and background seismicity within the ESRP is the most significant seismic hazard for the INTEC and CFA areas. Recent seismic hazards investigations specific to major INEEL facilities, including INTEC (Woodward-Clyde Federal Services [WCFS] 1996), have been performed. Ground motions expected in the area are not sufficient to cause a hazard for the relocated percolation ponds.

3.1.5 Volcanic Hazards

The most significant volcanic hazard in the proposed area is that due to inundation by potential future lava flows. Because the area is relatively remote from volcanic source areas to the southeast and southwest, the probability of inundation by lava flows is very low, in the range of 10^{-5} to 10^{-6} per year (Three Mile Island [TMI]-2 Independent Spent Fuel Storage Installation [ISFSI] Safety Analysis Report 1999). Considering the potential for mitigative actions, that probability may be reduced to below 10^{-6} per year.

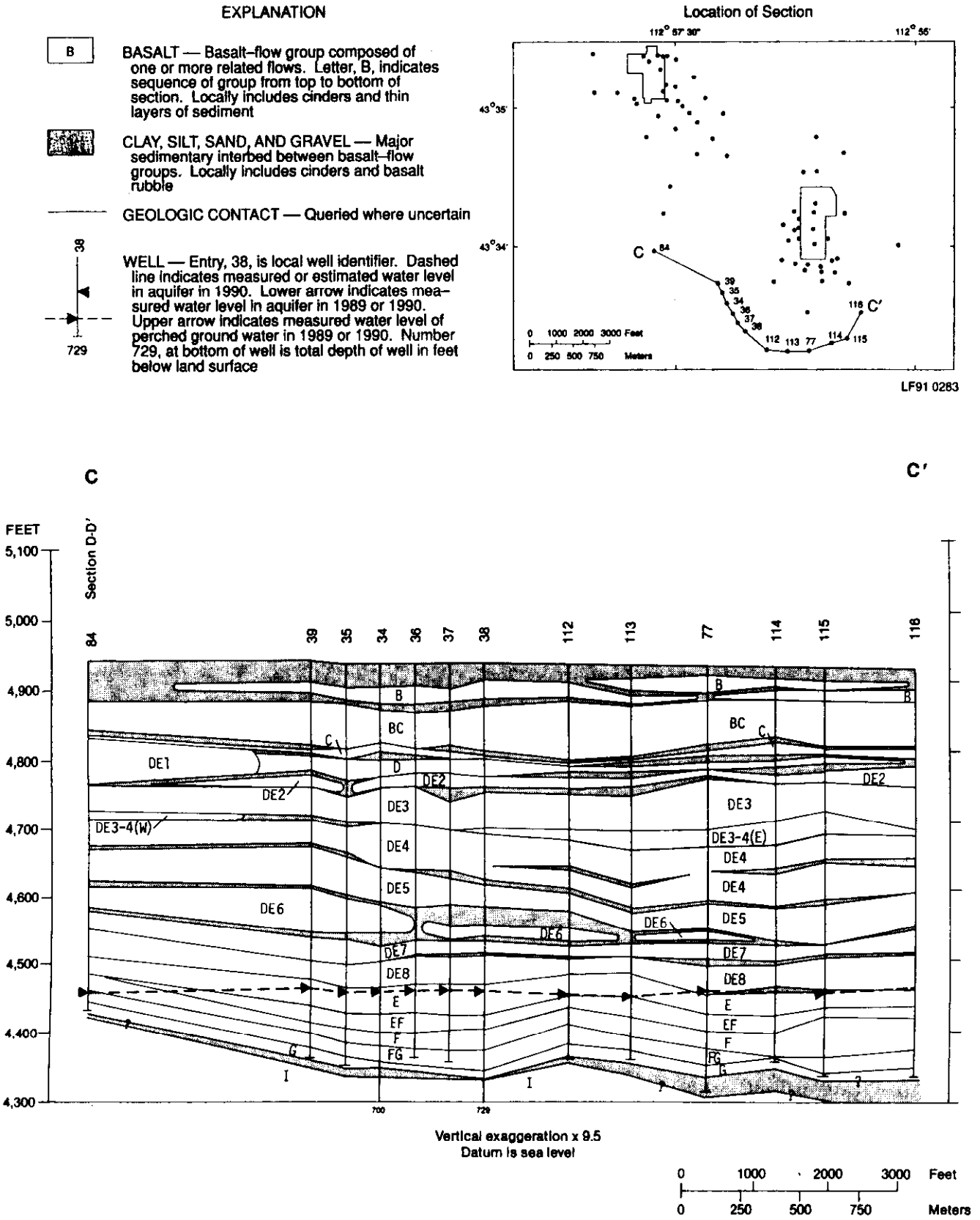

Figure 3-5. Geologic cross-section near INTEC (Anderson 1991).

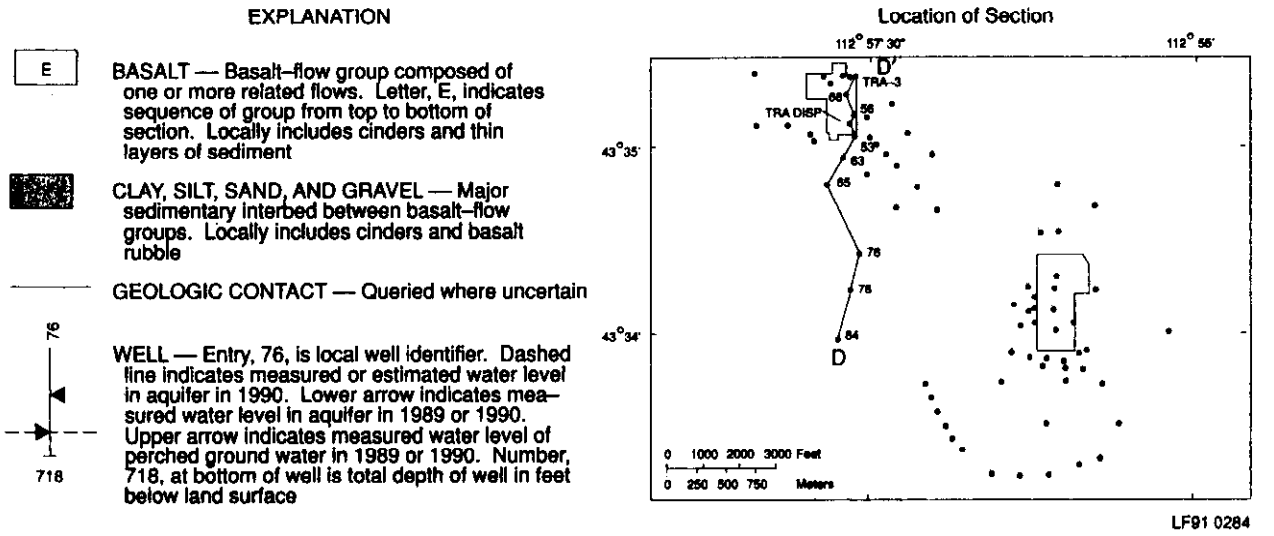

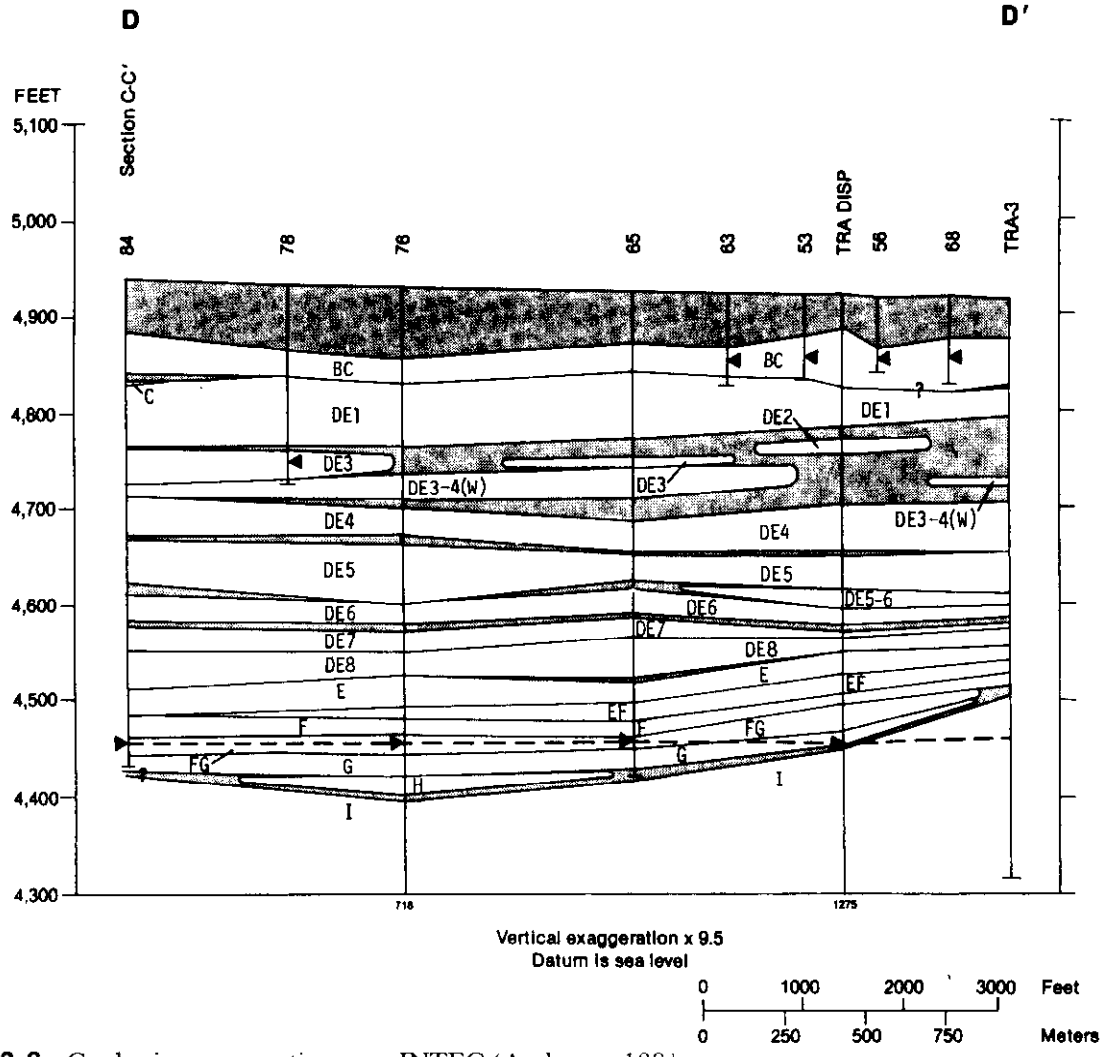

Figure 3-6. Geologic cross-section near INTEC (Anderson 1991).

3.2 Soils

In general, soils on the INEEL have formed by alluvial or eolian deposition over basalt lava flows and are derived from silicic volcanic and Paleozoic rocks from nearby mountains and buttes. The deeper soils are located in the central and northern portions of the Site, while shallower, rocky soils are generally found in the southern portion. Rock outcrops are common and some soils are relatively shallow.

Figure 3-7 depicts, in general, the soils typically found on the INEEL. The map constitutes an Order 4 or 5 soil survey as defined by the Natural Resources Conservation Service. The map conveys broad-scale landscape associations but lacks the detail necessary for facility siting. Complete descriptions of the mapping units and detailed descriptions of the soil series that compose the mapping units are provided in Olson et al. (1995).

Soils in the vicinity of the Big Lost River tend to be medium to coarse textured over gravel and are derived from alluvial deposits of the Big Lost River. These soils range from shallow, less than 51 cm (20 in.) to deep, more than 152 cm (60 in.). The cation-exchange capacity—an indicator of the ability of a soil to adsorb potential contaminants—ranges from 0 to 30 meq/100 g. Soils in the central portion of the INEEL tend to be moderately coarse-textured (from eolian sand) on basalt plains at depths ranging from shallow, less than 51 cm (20 in.) to deep, more than 152 cm (60 in.). The soils tend to have clay contents ranging from 2 to 35% and cation-exchange capacities ranging from 1 to 30 meq/100 g. Soils in the southern portions of the site tend to be medium- to fine-grained (from loess) on basalt plains and also are shallow to deep.

Soils within the area designated as the location for new percolation ponds are not characterized due to lack of site-specific data. Samples of alluvium will be collected during an engineering study scheduled for August or September 1999. The alluvial material will be described for hydrogeologic and engineering properties.

3.3 Surface Water Hydrology

The Big Lost River is the major natural surface water feature on the INEEL. Its waters, impounded and regulated by Mackay Dam (located approximately 81 km [50 mi] northwest of CFA in the Big Lost River Valley), flow from the dam southeastward through the Big Lost River Valley and onto the INEEL (see Figure 1-1). Streamflows are often depleted before reaching the INEEL by irrigation diversions and infiltration losses along the river. When flow in the Big Lost River actually reaches the INEEL, it is either diverted at the INEEL diversion dam (Figure 3-8) or flows northward across the INEEL in a shallow, gravel-filled channel passing within 0.8 km (0.5 mi) of the INTEC facility and the proposed pond location. After passing INTEC, the main channel branches into several channels 29 km (18 mi) northeast of the INEEL diversion dam, referred to as the Big Lost River Sinks and terminates in a series of three shallow playas that are connected by branching channels. All flow of the Big Lost River that enters onto the INEEL, except for evapotranspiration losses, is recharged to the subsurface. The stretch of the Big Lost River on the INEEL is ephemeral with no recreational or consumptive uses of the water.

The need for flood control on the INEEL was first recognized in the early 1950's when downstream facilities were threatened by localized flooding as a result of ice jams in the Big Lost River. The INEEL Diversion Dam was constructed in 1958 to divert high runoff flows from downstream INEEL facilities. The diversion dam consists of a small earthen dam and headgate that directs water from the main channel, through a connecting channel, and into a series of four natural depressions, called spreading areas. The capacity of the spreading areas is 58,000 acre-ft at an elevation of 1;539 m (5,050 ft) (McKinney 1985). An overflow weir in spreading area D allows water to drain southwest off the INEEL. Runoff from the Big Lost River has never been sufficient to exceed the capacity of the spreading areas and overflow the weir.

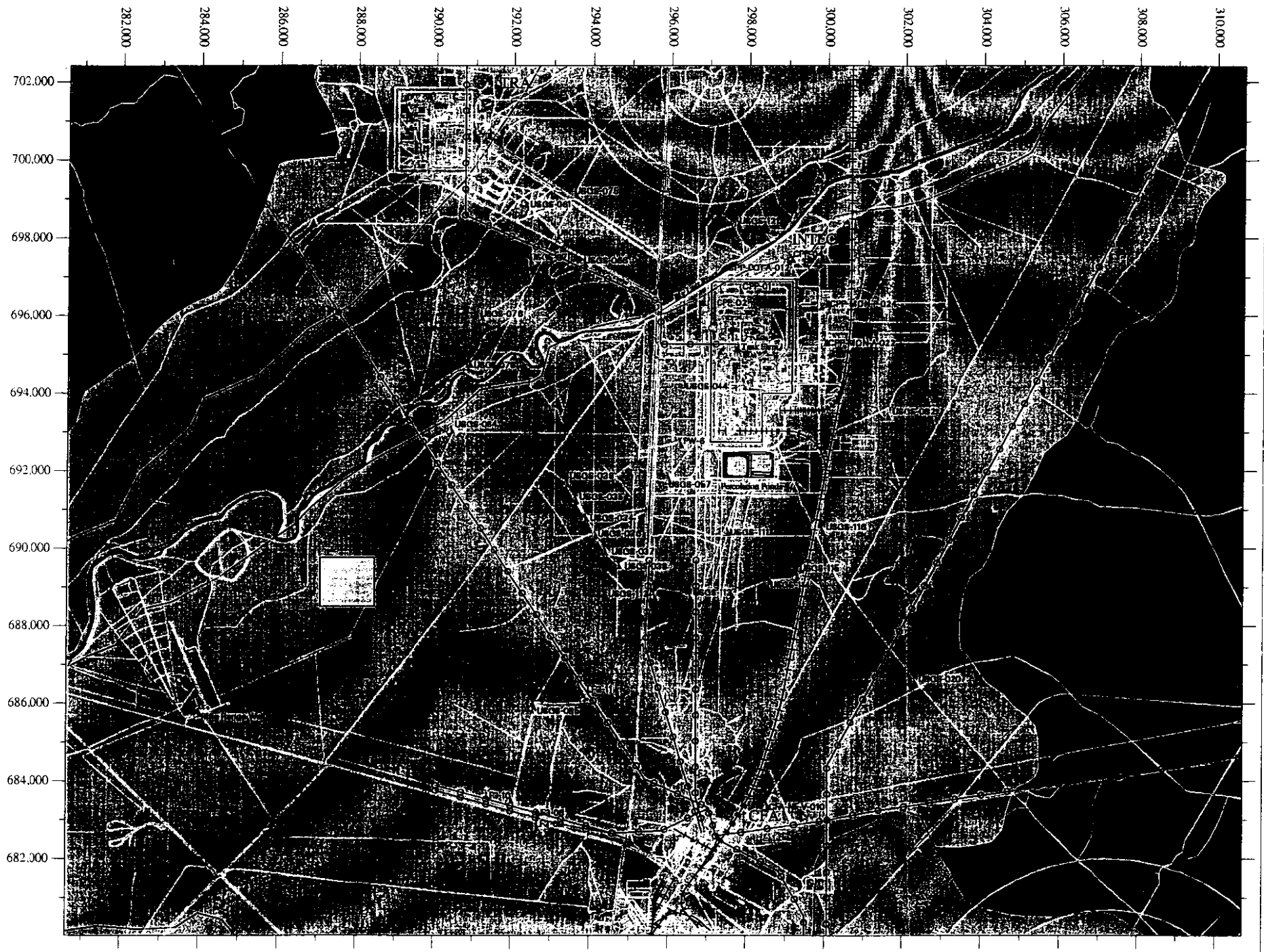

Surface Soils on the INEEL

N
W E
S

Legend

- Roads and Buildings
- Railroads
- Powerlines
- Existing Percolation Ponds, Tank Farm, INTEC Boundary
- Big Lost River
- Shallow to deep (<20" to >60") moderately coarse-textured soils (from eolian sand) on basalt plains with slope ranges from 0–20%
- Shallow to deep (<20" to >60") medium to fine grained soils (from loess) on basalt plains with slope ranges from 0–30%
- Shallow to deep (<20" to >60") medium to coarse textured soils over gravel: derived from alluvial deposits of the Big Lost River and Birch Creek
- Approximate New Percolation Pond Area
- Well Locations

Description: General depiction of soils typically found on the INEEL. The map constitutes an Order 4 or 5 soil survey as defined by the Natural Resources Conservation Service. The map conveys broad-scape associations but lacks the detail necessary for facility siting.

Reference: Olson, G.L., D.J. Jeppesen, and R.D. Lee, January 1995, The Status of Soil Mapping for the Idaho National Engineering Laboratory, INEL–95/0051, Lockheed Martin Idaho Technologies Company.

0 1 2 3 km

0 1 2 Miles

Date Drawn: September 20, 1999

INEEL SPATIAL ANALYSIS LABORATORY

APPLYING TECHNOLOGY TO MEET ENVIRONMENTAL NEEDS

(/projects/cpp/new_perc_pond_maps: soils_general_base-bi_v1)

Figure 3-7. Surficial soil units mapped on the INEEL.

NOTES: With the exceptions noted below, all hydrological features are based on DLG electronic data for 1: 24,000 scale maps obtained from the USGS.

1. Spreading Areas: Boundaries were delineated using July 1984, Landsat TM imagery which shows these areas full of water. The edge of the water was identified and digitized on screen to create the boundary file.

2. Playa No. 1: The USGS 1: 24,000 scale DLG electronic data for Playa No. 1 was arbitrarily extended over the INEEL boundary on the west side of the playa to indicate that irrigation water is taken at this point.

3. Playa No. 4: Ron Rope August 30, 1996, Interoffice Correspondence to Dennis Walker transmitting the Playa 4 Delineation Study information.

4. Hydrological features for the following USGS 7.5' Quads were digitized by Lowell Williams and Marci Cook in June 1992:

   A. Kettle Butte N.W.
   B. Kettle Butte S.W.
   C. Quaking Aspen Butte
   D. Richards Butte
   E. Terreton
   F. Scoville
   G. Big Southern Butte

5. Birch Creek Diversion: Survey data from Sorensen Engineering, Idaho Falls, Idaho, February 1988, Birch Creek Hydroelectric Facility, Drawing No. D88-13429. Birch Creek Diversion includes the irrigation return flow from Reno Ranch.

6. Roads and Facilities: Based on digital data obtained from Aerial Mapping, 1993.

7. These areas include features mapped by the USGS, Fish and Wildlife Service National Wetlands Inventory, and INEEL personnel. Some areas characterized during field investigations are described in the following documents:
   Hampton, N.L., R. C. Rope, L. M. Glennon, and K. S. Moor. A Preliminary Survey of the National Wetlands Inventory as Mapped for the Idaho National Engineering Laboratory, February 1995. INEL–95/0101. National Technical Information Service, Springfield, Virginia.
   Rope, R. C., B. J. Grizzle, N. L. Hampton, J. A. Tullis, and J. M. Glennon. Characterization and Distribution of INEL Wetlands and Playas, Draft Report, September 1996.

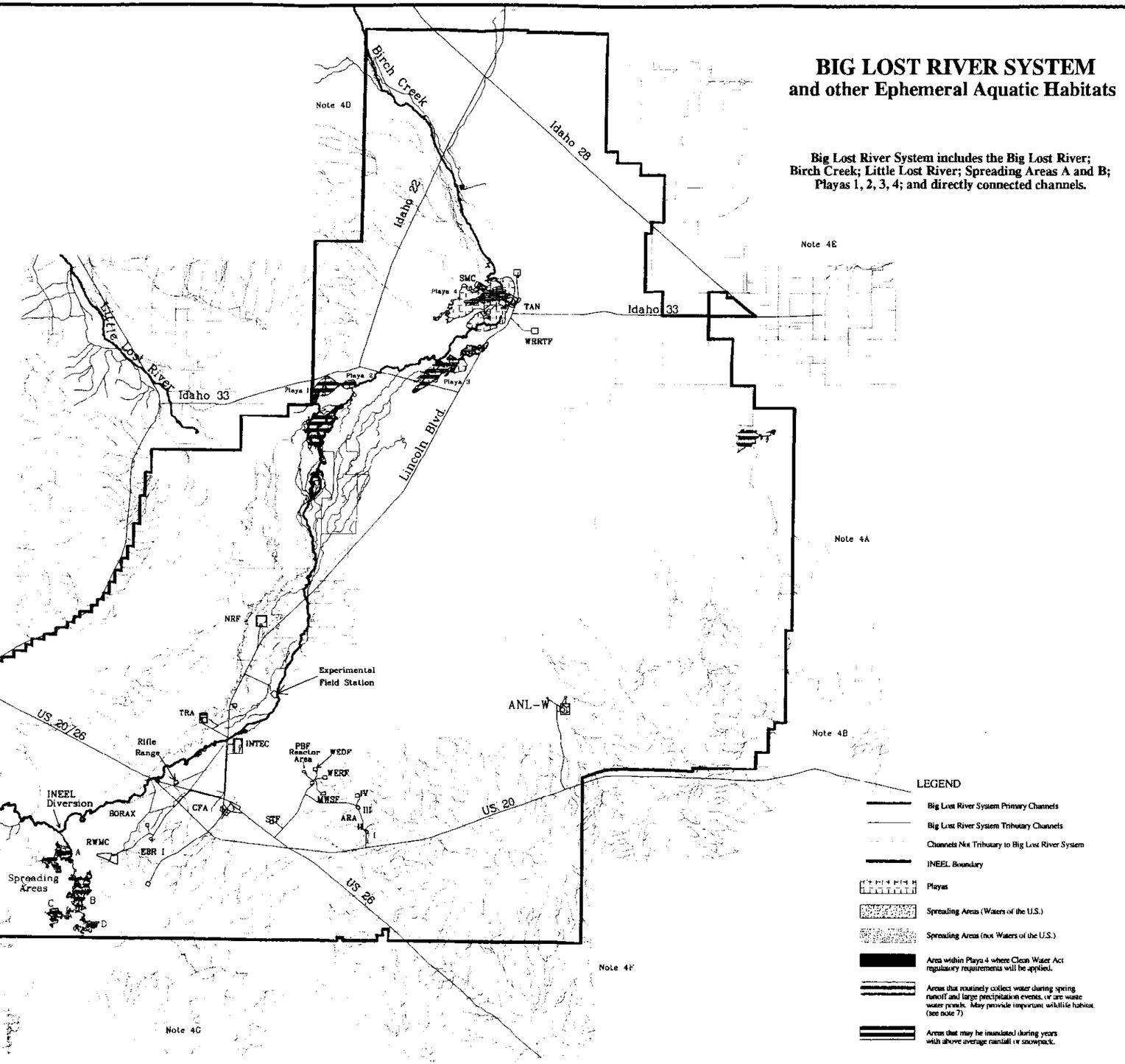

Figure 3-8. Channels and flow paths of the Big Lost River both off and on the INEEL.

3.3.1 Big Lost River 100-Year Floodplain

Several studies have presented estimates of the potential magnitude of the 100-year flood for the Big Lost River, some of which are discussed below. The 100-year flood for the Big Lost River near Arco, a station 23 km (14 mi) upstream from the INEEL diversion dam, has an estimated magnitude of approximately 3,700 to 4,400 cfs based on a log-Pearson Type III distribution of historical stream gaging records (Tullis and Koslow 1983; U.S. Army Corps of Engineers 1991; and Stone, Mann and Kjelstrom 1992). Another study used a log-Pearson Type III distribution for a station upstream of Mackay Reservoir combined with a regional regression approach for 22 subbasins and estimated a peak flow of 7,200 cfs for the 100-year flood for the Big Lost River at the Arco station (Kjelstrom and Berenbrock, 1996). This estimate is considered to be conservatively high. The highest recorded flow at the Arco station was 1,890 cfs in July 1967. A recent study using paleohydrologic data collected from several stream reaches along the Big Lost River below the Arco station in combination with historical stream gage data from the Arco station, and a Bayesian flood-frequency analysis estimates a magnitude of 3,300 cfs for the 100-year flood for the Big Lost River at the Arco station (Ostenaa et al. 1999). This latest study which combines historical streamflow data with paleohydrologic field study sites along the Big Lost River provides the best estimate of the 100-year flood to date. Therefore, a reasonable estimate of the 100-year flood for the Big Lost River at the Arco station is considered to be 3,300 cfs.

The INEEL diversion dam controls flow onto the site protecting downstream facilities (Figure 3-8). Gates placed on two large, corrugated steel culverts control flow onto the Site; less than 900 cfs of flow is released through the diversion dam, downstream onto the INEEL (Lamke 1969). The INEEL diversion channel is capable of handling flows in excess of 7,200 cfs (Bennett 1986). However, a recent field investigation pertaining to the structural integrity of the INEEL diversion dam by the Army Corps of Engineers indicates sustained flows of 7,200 cfs (diversion dam capacity with no freeboard) could damage or overtop the dam.[b] The report indicates dam failure is possible at flows in excess of 6,000 cfs. The safe holding capacity of the diversion dam with a minimum freeboard of 0.9 m (3 ft) is now thought to be about 5,000 cfs. The controlled flow of the Big Lost River downstream on the INEEL and the lack of additional contributing flows to the river on the INEEL indicate the 100-year flood (3,300 cfs) on the Big Lost River would be contained within the natural channel and diversion channel, posing no flood threat to INEEL facilities.

A USGS floodplain study (Berenbrock and Kjelstrom 1998) routed their conservatively high estimate of the 100-year peak flow (7,200 cfs) (Kjelstrom and Berenbrock 1996) downstream onto the INEEL (Figure 3-9). The flood-routing study did not include the INEEL diversion dam in the model simulation. The study assumes 1,000 cfs of the peak flow will flow down the diversion channel and the remaining flow of 6,200 cfs is routed downstream onto the INEEL using a one-dimensional code that does not account for infiltration, side or overbank losses. This conservative floodplain study indicates a potential for flooding in the north end of INTEC. However, evaluation of the INTEC geomorphic setting based on soil profiles along the Big Lost River that were used to develop a late Quaternary soil chronosequence indicates that INTEC is sited on geomorphic surfaces that are well in excess of 10,000 years in age, an indication that the hazard of significant flooding of this area by the Big Lost River is low under natural channel conditions (Ostenna et al. 1999).

---

[b] R. M. Berger, Draft memorandum, *Draft Plan of Study Big Lost River Diversion Dam and Facilities*, U.S. Army Corps of Engineers, Walla Walla District, June 17, 1997.

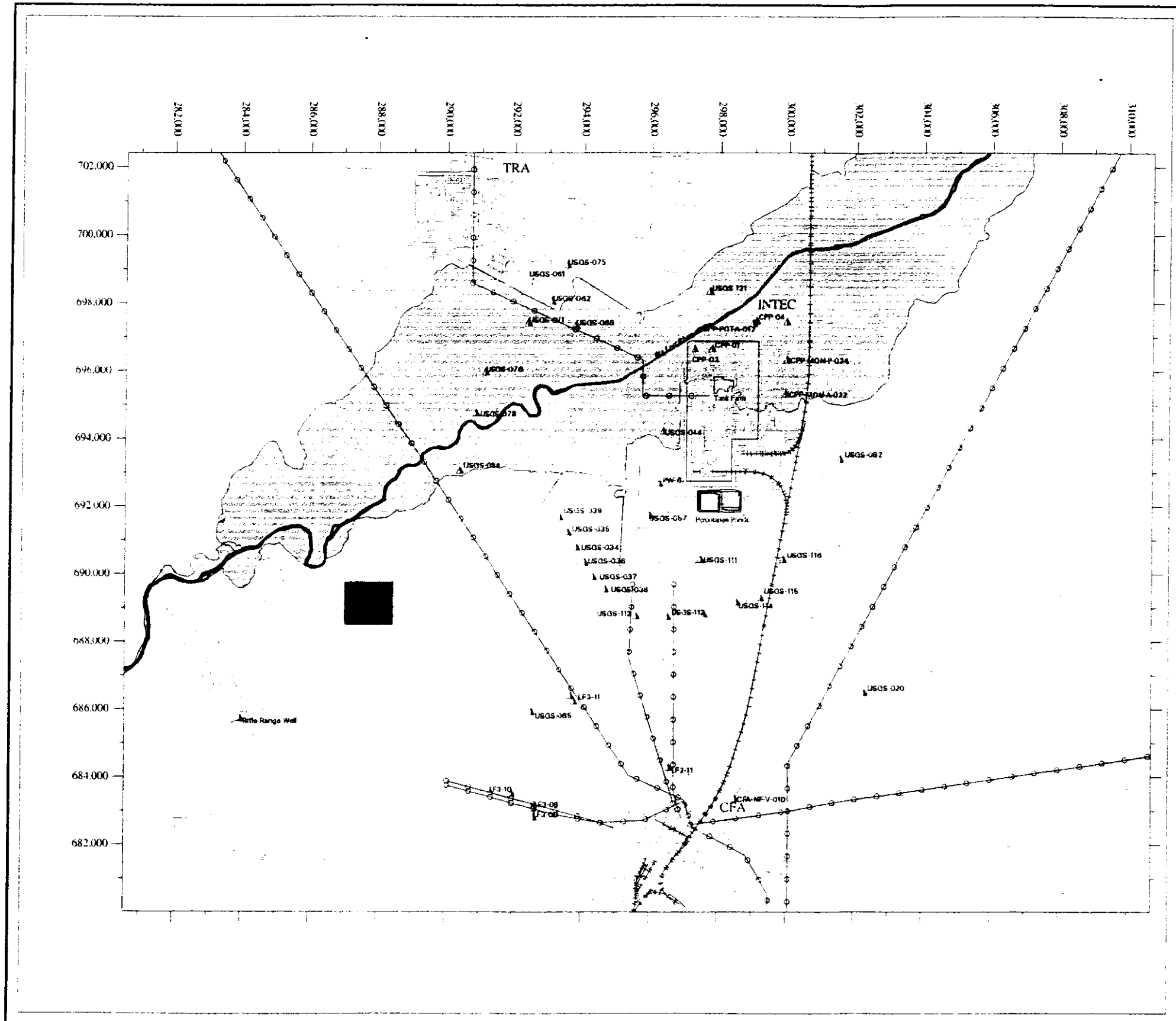

USGS Big Lost River 100- Year Flood Plain

N
W E
S

Legend

- Roads and Buildings
- Railroads
- Powerlines
- Existing Percolation Ponds, Tank Farm, INTEC Boundary
- Big Lost River
- USGS 100 Year Flood Plain
- Approximate New Percolation Pond Area
- Well Locations

Note: 500–year or 1000–year flood plain boundaries have not been designated.

Reference:

Kjelstrom, L.C. and C. Berenbrock, 1996, "Estimated 100–Year Peak Flows and Flow Volumes in the Big Lost River and Birch Creek at the Idaho National Engineering and Environmental Laboratory, Idaho.", Water Resources Investigations Report 96–4163, U.S. Geological Survey.

0 1 2 3 km

0 1 2 Miles

Date Drawn: September 20, 1999

INEEL SPATIAL ANALYSIS LABORATORY

APPLYING TECHNOLOGY TO MEET ENVIRONMENTAL NEEDS

\\projects\cpp\new_jets_pond_maps\flood_100yr_and_base-bl_v1

Figure 3-9. USGS Big Lost River 100-year flood plain.

3.3.2 Big Lost River Floods with Return Periods Greater Than 100 Years

Ostenna et al. (1999) performed a Bayesian flood-frequency analysis that indicates peak flows on the Big Lost River with return periods of 500, 1,000, and 10,000 years are 4,000, 4,400,and 5,300 cfs, respectively. These results suggest that exceedance of the estimated maximum capacity of the INEEL diversion dam of 9,300 cfs (Bennett 1986) has an extrapolated annual exceedance probability smaller than 0.00001 (or greater than the 100,000 year return period). Assuming a safeholding capacity of 5,000 cfs for the INEEL diversion dam the annual exceedance probability is 0.0002 (or a 5,000 year return period).

3.3.3 Recent Localized Flooding

In approximately 1962, late winter frozen ground coupled with rapid snowmelt resulted in ponded water at the CFA facility. In order to drain the water and prevent a similar reoccurrence, a series of drainage ditches or canals were excavated to the north and northwest of the CFA. Many of these ditches are located within the vicinity of the proposed location.

3.4 Subsurface Hydrology

This subsection describes the vadose zone, perched water bodies, and the groundwater at INTEC. Regional descriptions can be found in Holdren et al. 1997 and DOE-ID 1997.

3.4.1 Vadose Zone

The hydraulic properties of the vadose zone underlying INTEC (basalt layers and sedimentary interbeds) are not fully characterized. However, some hydraulic properties for various components of this zone have been determined and are summarized below. Bishop (1991) measured several hydraulic properties of vesicular basalt cores obtained at the RWMC. The mean horizontal and vertical saturated hydraulic conductivities were 8.42E-06 and 9.81E-05 cm/s (0.02 and 0.28 ft/day), respectively. The effective porosity was 23%. Moisture characteristic curves indicated that more than 90% of the moisture was lost during drainage from 0 to 100 kPa tension. D. B. Stephens and Associates (1993) measured several hydraulic properties of a shallow sedimentary interbed between CFA Landfills II and III. The hydraulic properties reflect the generally coarse nature of these sediments. However, considerable variation exists in these properties (e.g., the saturated hydraulic conductivity varies by more than three orders of magnitude at a range of 9.8E-06 to 4E-02 cm/s (0.027 to 113 ft/day), and moisture retention at 15,000 cm H_2O varies from 5.3 to 21.9% [cm^3/cm^3]).

The movement of water through thick sequences of basalt flows and sedimentary interbeds can be relatively rapid during periods of saturation. Morris et al. (1963) observed the rise of the water table at a depth of about 142 m (465 ft) in Well 5 about 15 to 20 days after the beginning of runoff from the rapid spring thaw in 1962. The water table rose from 142 m (466 ft) bls to about 141 m (463 ft) bls. Barraclough et al. (1967) reported that the water level in Well 78, which was 62 m (203 ft) deep and 72 m (235 ft) from the Big Lost River, started to rise within 4 days after the water first flowed into the Big Lost River channel. Pittman et al. (1988) reported that water levels in some wells at the INEEL rose as much as 1.8 m (6 ft) or more in a few months following high flows in the Big Lost River. In a large field experiment, water infiltrating from a 2.6-ha (6.6-acre) circular pond advanced vertically through the basalt vadose zone at a rate of about 6.0E-03 cm/s (15.2 ft/day) (Wood and Norrell 1996).

Moisture movement through the vadose zone at the INEEL during unsaturated conditions would be significantly slower than these observations suggest and would depend on the amount of infiltrating water and the moisture content of the vadose zone materials. The same material features (e.g., open fractures

and large pores within the basalt) that contribute to rapid flow during saturated conditions impede moisture movement under unsaturated conditions.

Hydrologic properties testing has been performed on nine wells completed in the upper perched zone beneath INTEC. Field tests were conducted on basalt and the 33.5 and 42.7-m (110 and 140-ft) sedimentary interbeds to determine horizontal hydraulic conductivities. Laboratory tests were conducted on samples for the 33.5-, 42.7-, and 70.1-m (110-, 140-, and 230-ft) interbeds to determine vertical hydraulic conductivities. Table 3-1 presents the results of the field laboratory tests. The horizontal hydraulic conductivity values are higher than the vertical conductivity values, which may be expected due to depositional features which favor lateral hydraulic movement over vertical movement. However, it is also possible that the field tests were measuring the effects in the basalt as well as the sediments. Table 3-1 presents a summary of the field data and laboratory hydraulic conductivity measurements (Appendix A and DOE-ID 1997).

Site-specific hydraulic properties of the vadose zone beneath the proposed location of the new INTEC facility are not characterized. The wastewater land application permit proposes the installation of four new aquifer wells and six perched water wells with the combined purpose of providing site-specific characterization data and groundwater monitoring capabilities.

3.4.2 Perched Water

Lithologic features contributing to contrasts in the saturated vertical hydraulic conductivity of basalt layers and sedimentary interbeds in the unsaturated zone provide mechanisms for the development of perched groundwater bodies. Perched groundwater zones at TRA, INTEC, TAN, and the RWMC can be attributed to at least four lithologic features:

1. The vertical hydraulic conductivity of a sedimentary interbed is often lower than that of an overlying basalt flow.

2. Alterations in the baked zone between two flows can contribute to reduced vertical hydraulic conductivity.

3. Dense unfractured basalt may inhibit moisture movement, which would contribute to the formation of perched water zones.

4. Sedimentary and chemical filling of fractures near the upper contact of a basalt flow reduces the vertical hydraulic conductivity.

In Feature 1, the saturated horizontal hydraulic conductivity of basalts in the unsaturated zone at the INEEL may range from 3.0E-04 to 2.5 cm/s (1 to 7,000 ft/day) (Robertson 1977). Saturated vertical hydraulic conductivity of sedimentary interbeds may range from 3.5E-09 cm/s (1.0E-05 ft/day) near the RWMC to 2.4E-03 cm/s (7 ft/day) in playa sediments in the northern part of the INEEL (Robertson 1977). Generally, horizontal hydraulic conductivity of basalts is larger than the vertical hydraulic conductivity. The smaller vertical hydraulic conductivity of a sedimentary interbed underlying a more permeable basalt layer impedes the movement of water and contributes to the formation of a perched groundwater zone.

Table 3-1. Summary of field and laboratory hydraulic conductivity for basalt and interbeds at INTEC (Appendix A and DOE-ID 1997).

Material	Depth (ft)	Field Hydraulic Conductivity ($Ksat_{hor}$) (cm/sec)	$Ksat_{vert}$ (cm/sec)	Laboratory $Ksat_{vert}$ (cm/sec)
Basalt		9.5E-04 to 1.3E-03	3.7E-05 (3.0E-07 to 2.1E-03)	NA
CD interbed (range)	110	3.9E-05 to 1.8E-03	1.3E-04 (5.2E-08 to 3.4E-03)	3.0E-07 to 2.1E-03
D interbed (range)	140	1.3E-03	3.3E-04	5.2E-08 to 3.4E-03
Deep interbed (range)	230	N/A	1.4E-06 (1.7E-08 to 1.4E-03)	N/A

In Feature 2, the intense heating of the upper surface of an existing flow from the emplacement of an overlying flow causes oxidation of glassy matrix and olivine crystals and coats scoria fragments, vesicles, and fracture surfaces with iron oxides and iron hydroxides (Kuntz et al. 1980). These baked-zone alterations can modify the orientation and dimensions of fractures in the underlying flow, which would reduce vertical hydraulic conductivity. The extent of alteration and its effect on vertical flow can be influenced by the presence of sediment and water at the time of emplacement, the temperature of the overlying magma, and other factors (Cecil et al. 1991).

In Feature 3, lithologic, geophysical, and borehole video logs from wells at the INEEL indicate that some basalt flows are dense and unfractured. The absence of fractures decreases the vertical hydraulic conductivity of the basalts contributing to the formation of perched groundwater zones.

In Feature 4, the efficiency by which water is transmitted through fractures is dependent on aperture width, wall irregularity, attitude, and interconnection of fractures. Sedimentary materials accumulate in fractures during sediment aggradation onto a basalt surface, which reduces the water-transmitting efficiency of a fractured matrix (Cecil et al. 1991). Post-depositional fracture filling continues as infiltrating water transports sediment. During periods of major recharge, sediment transported by infiltrating water may include coarse silt and fine sand, but fine clay fractions are preferentially deposited. Most fracture filling occurs in the upper 0.9 m (3 ft) of a basalt flow (Cecil et al. 1991). Calcium carbonate also precipitates on fracture walls, which reduces the fracture size and decreases the capability of the fractured matrix to transmit water. Researchers have observed that carbonate was concentrated in fractures in the uppermost 4.8 m (16 ft) of a basalt flow at the RWMC (Cecil et al. 1991).

Perched water bodies have formed beneath all INEEL infiltration ponds. The geohydrologic characteristics of the unsaturated zone underlying TRA, INTEC, TAN, and the RWMC differ with respect to basalt and sediment lithology, unit thickness, and physical orientation. These facilities also differ in the volumes of effluent discharged to the infiltration ponds, the sizes of the area over which recharge occurs, and the degree of saturation both horizontally and vertically. Although these differences exist, the features that control the formation of perched groundwater zones are common to the four facilities.

The discharge of wastewater into two infiltration ponds at INTEC caused perched groundwater zones to form in the vicinity of the ponds. Other sources of infiltration contributing to the formation of

perched water include the sewage treatment ponds, water system leaks, landscape irrigation, precipitation, steam condensate, CPP-603 basins, and the Big Lost River. The complex stratigraphy beneath INTEC is poorly understood. The lithologic record of USGS Well-51, located at the northwest corner of Pond 2, indicates that as many as 13 basalt flow groups and six sedimentary interbeds exist in the vadose zone beneath the ponds. At least four perched groundwater zones have been identified beneath the infiltration ponds. These include a zone of saturation in the surficial alluvium and three separate zones in the underlying basalt and sedimentary interbeds. By 1986, perched groundwater zones had formed at USGS Well-51, located at the northwest corner of Pond 2, at depth intervals from 9 to 31 m (30 to 104 ft), 40 to 54 m (134 to 178 ft), and 80 to 98 m (266 to 322 ft). A thin perched groundwater zone formed at the surface alluvium-basalt interface because the alluvium is relatively more permeable than the underlying basalt (Cecil et al. 1991). The lateral extent of this body approximates the pond boundaries and is assumed to be dominated by vertical infiltration. Deeper perched water zones have been identified in the basalt at depths between 34 and 52 m (113 and 170 ft) bls and 97 and 128 m (320 and 420 ft) bls. The approximate extent of the 34-m (110-ft) perched zone is shown in Figure 3-10. Some of the perched water wells completed in the area between the existing percolation ponds and the tank farm are wet and some are dry, indicating either a lack of perched water, a slightly less than 100% saturation resulting in the lack of standing water in the well, or the possibility of discontinuities in the interbeds. No information is available about the soil moisture content in the "dry" wells.

Of particular interest for this siting study is the lateral extent of the perched water bodies beneath the existing ponds. This is needed to provide an estimate based on real data for the lateral extent of perched water expected to form from discharges to new ponds. Although the stratigraphy at the new location may differ, an approximation of the behavior of infiltrating water can be assumed. Modeled results presented in DOE-ID 1997 (WAG 3 OU 3-13), suggested that lateral spread on the 34-m (110-ft) interbed is large. However, the perched water bodies beneath INTEC are neither well understood nor quantified because of a lack of needed data and the conflicting nature of existing data. Ideally, regular water level and chemical composition monitoring are needed to observe trends in the water levels and chemistry to defensibly understand the perched water body interactions.

3.4.2.1 Estimated Extent of Perched Water from New Percolation Ponds. It is a basic assumption that perching of percolation pond infiltrate at relocated disposal ponds will occur similarly to that observed at the existing ponds. Because of this, it is of primary interest whether perched water due to the relocated ponds will extend to the perched water zones beneath the existing ponds. Additionally, this information is critical to determine WLAP-regulated facility boundaries and impacts to adjacent areas such as wellhead protection zones and the Big Lost River, and to ensure that aquifer monitoring wells are located correctly to measure impacts to groundwater from operation of the facility.

WAG 3 OU 3-13 modeling for a 1.5 mg/day discharge to the existing ponds predicts the lateral spread of 100% saturation to be 549 m (1,800 ft) from the center of the existing ponds (Figure 3-11). The estimated 90% saturation boundary for the same discharge volume is 1,555 m (5,100 ft). For the new percolation ponds, an increased discharge volume (3 MG/day) coupled with the OU 3-13 model parameters predicted a lateral spread of perched water (100% saturation) to be 1,219 m (4,000 ft) from the center of new ponds. The 90% saturation boundary extended to 1,890 m (6,200 ft) from the same point. Also shown in Figure 3-11, the OU 3-13 modeled radii suggest that there will be an impact from the new ponds on the perched water associated with the existing ponds. However, it is assumed that there will be no impact to the existing perched water from new pond discharged because: (1) the OU 3-13 WAG 3 model is extremely conservative, (2) there is a long time interval before the new ponds will receive 3 MG/day of waste water, (3) the measured perched water extent beneath the existing ponds is smaller than the OU 3-13 modeled extent, and (4) there is a 3-km (2-mi) separation between the existing ponds and the new ponds.

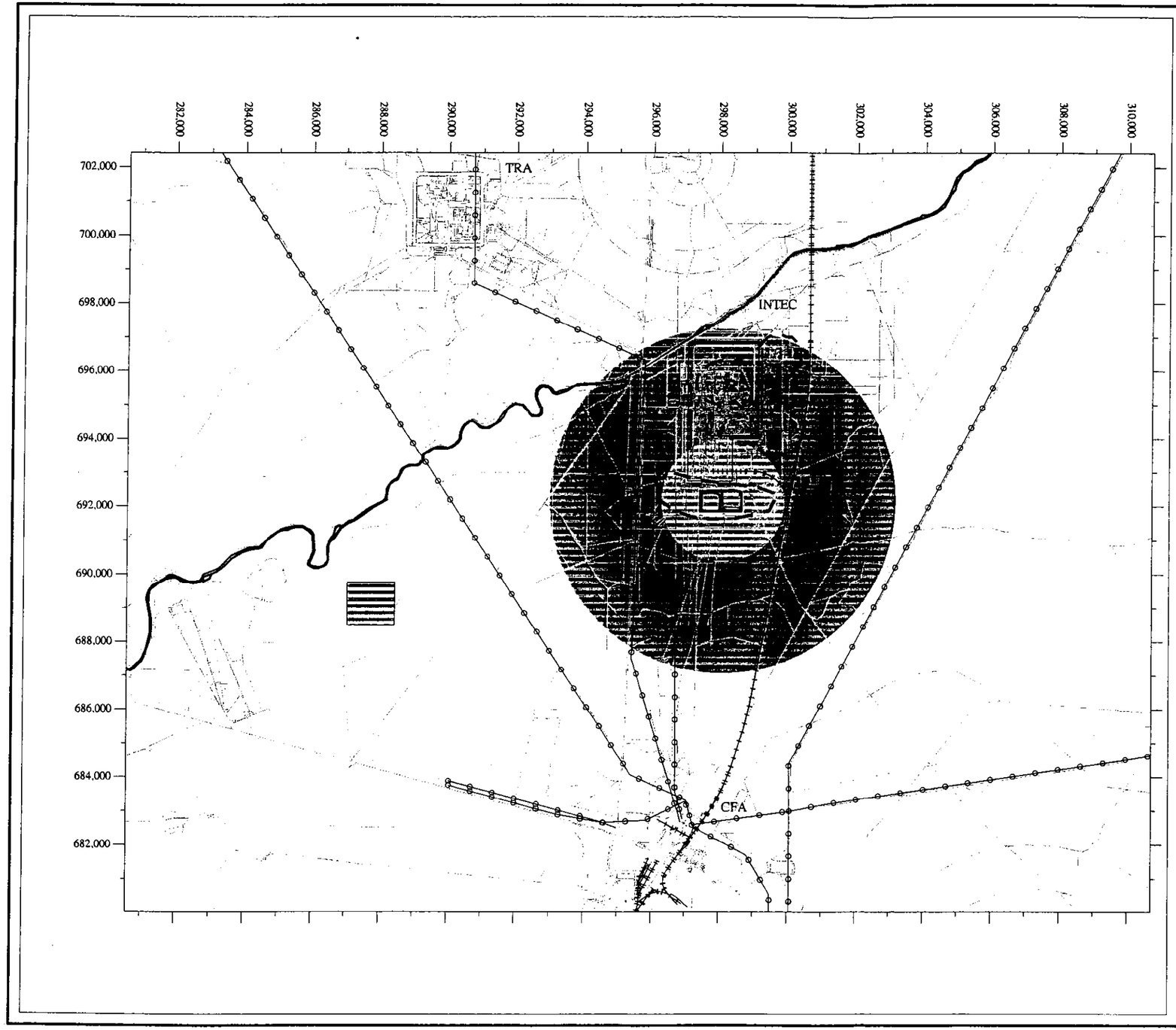

Measured and WAG-3 OU3-13 Modeled Extent of Perched Water Beneath INTEC

N
W E
S

Legend

- Roads and Buildings
- Railroads
- Powerlines
- Percolation Ponds, Tank Farm, INTEC Boundary
- Big Lost River
- INTEC Perched Water Contours (measured)
- Approximate New Percolation Pond Area
- Modeled extent of perched water, OU 3–13 parameters, 1.5 MGD, 110' Interbed, 100% saturation
- Modeled extent of perched water, OU 3–13 parameters, 1.5 MGD, 110' Interbed, 90% saturation

Reference:

DOE/ID, "Comprehensive RI/FS for the Idaho Chemical Processing Plant OU3–13 at the INEEL – Part A. RI/BRA Report (Final)", U.S. Dept. of Energy DOE/ID–10534, November 1997.

0 1 2 3 km

0 1 2 Miles

Date Drawn: September 20, 1999

INEEL SPATIAL ANALYSIS LABORATORY

APPLYING TECHNOLOGY TO MEET ENVIRONMENTAL NEEDS

(/projects/spp/new_perc_pond_maps: interbed_basemap-bl_v3)

Figure 3-10. Measured and WAG 3 OU 3-13-modeled extent of perched water beneath INTEC.

WAG-3 OU3-13 Modeled Lateral Extent of Perched Water Beneath INTEC and the Proposed Location of New Percolation Ponds

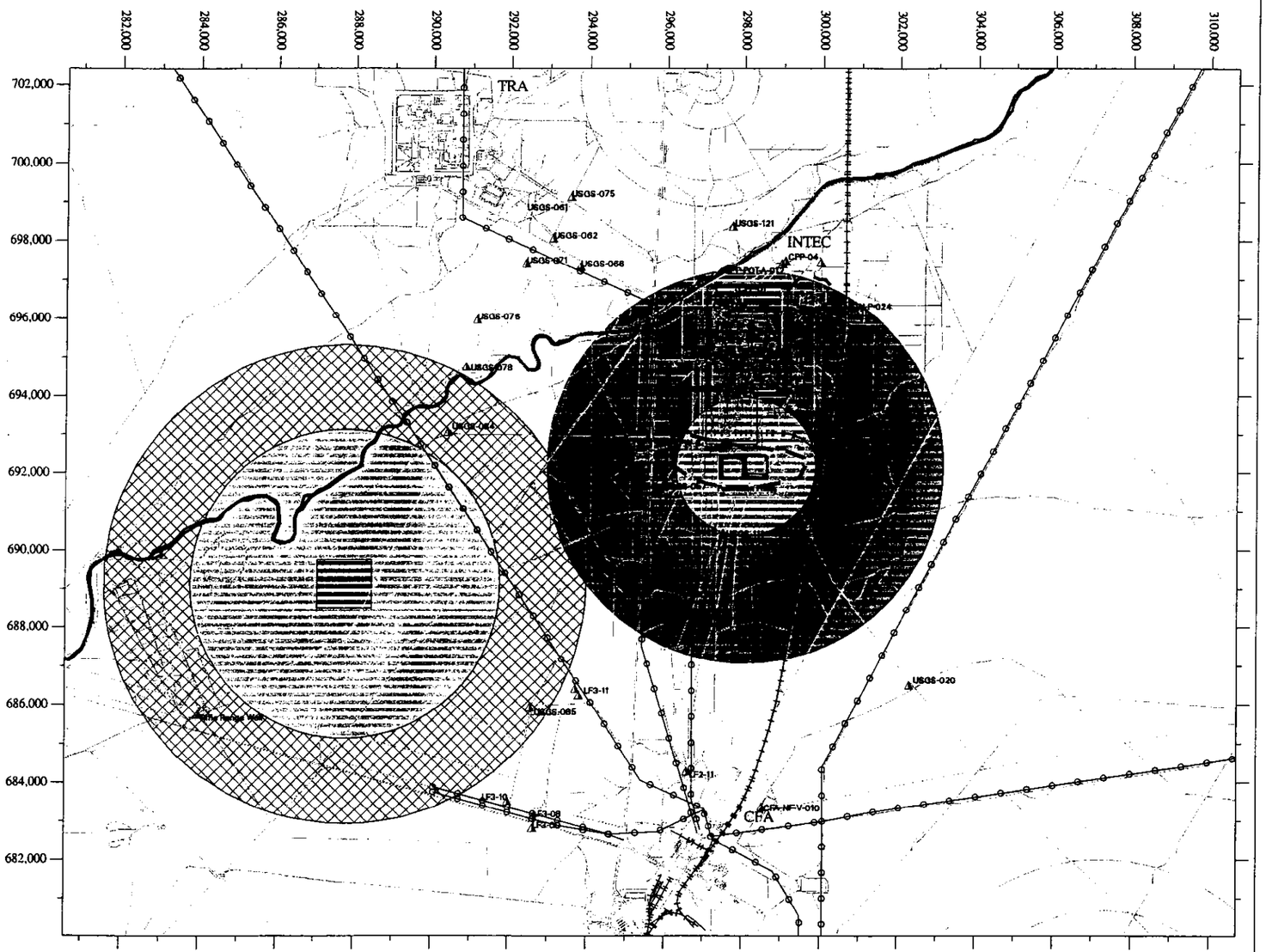

Legend

- Roads and Buildings
- Railroads
- Powerlines
- Existing Percolation Ponds, Tank Farm, INTEC Boundary
- Big Lost River
- INTEC Uppper Perched Water Contours, measured in 110' and 135' interbeds
- Well Locations
- Approximate New Percolation Pond Area
- Modeled extent of perched water, OU 3–13 parameters, 3 MGD, 110' Interbed, 100% saturation
- Modeled extent of perched water, OU 3–13 parameters, 3 MGD, 110' Interbed, 90% saturation
- Modeled extent of perched water, OU 3–13 parameters, 1.5 MGD, 110' Interbed, 100% saturation
- Modeled extent of perched water, OU 3–13 parameters, 1.5 MGD, 110' Interbed, 90% saturation

Reference:

DOE/ID, "Comprehensive RI/FS for the Idaho Chemical Processing Plant OU3–13 at the INEEL – Part A. RI/BRA Report (Final)", U.S. Dept. of Energy DOE/ID–10534, November 1997.

0 1 2 3 km

0 1 2 Miles

Date Drawn: September 20, 1999

INEEL SPATIAL ANALYSIS LABORATORY

APPLYING TECHNOLOGY TO MEET ENVIRONMENTAL NEEDS

(/projects/cpp/new_perc_pond_maps: perc_pond_contours-bl_v1)

Figure 3-11. WAG 3 OU 3-13-modeled lateral extent of perched water beneath INTEC and the proposed location of new percolation ponds.

A second critical reason to estimate lateral spread of perched water from the new ponds is to comply with State of Idaho and Federal regulations that there be no impact to groundwater from new facilities. Theoretically, the point at which impact is measured is a distance downgradient of the intersection between the infiltrate and the aquifer. From other INEEL perched water analogs (INTEC, TRA, TAN, and RWMC), the behavior of perching water in the vadose zone can be summarized as primarily downward migration through the surficial alluvium and downward until a lesser permeable zone is encountered. At that point, horizontal flow becomes dominant creating a perched water body. When hydraulic head and horizontal flow equilibrate, downward flow again becomes dominant across the area of the perched water body. This predominantly downward movement continues to the aquifer with minor additional spreading occurring when other less permeable zones are encountered. Therefore, the area of contact between infiltrate and the aquifer surface is approximated by the area of the perched water body, not the area of the disposal ponds. In order to accurately measure what, if any, impact there is to the aquifer from the new ponds, monitoring wells must be located downgradient of the lateral boundary of the perched water body, not within the boundary or excessively far away.

In conclusion, the OU 3-13-modeled 100% saturation boundary of 1,219-m (4,000-ft) radius almost certainly overestimates lateral spreading because of several excessively conservative model parameters and assumptions. Consequently, the OU 3-13 model is not appropriate to use as a guide for locating aquifer monitoring well locations. A modification of the OU 3-13 model predictions is required to design a groundwater monitoring network that ensures groundwater impacts are accurately detected. An aquifer and perched water monitoring network is proposed in the WLAP application.

3.4.3 Snake River Plain Aquifer

The SRPA, one of the most productive aquifers in the United States (Lindholm 1981), was classified as a sole-source aquifer by the EPA in 1991. The aquifer flow embedded within the basalt stratigraphy of the Snake River Plain is governed by the structure of individual basalt layers. Horizontal movement of water within the aquifer, the predominant movement direction, is aided by hydraulically connected interflow zones created by the upper vesicular zone of a basalt flow coupled with the fractured and often rubbly substratum of the overlying flow. Vertical movement of water, controlled by pore size, fracture size, and fracture density, is generally limited within the dense interior elements of a flow. Fracture joints in the central portion of the lava flow are typically vertical in orientation. As discussed earlier, although these vertical fractures are believed to serve as the primary means for vertical groundwater movement, they may actually lead to little vertical or horizontal movement of groundwater flow due to sedimentary and chemical infilling of fractures and alteration zones. Further contributing to the reduction of vertical flow is the presence of sedimentary interbeds. These interbeds, typically composed of fine-grained, clayey materials, have hydraulic conductivities 3 to 5 orders of magnitude lower than that of the surrounding fractured basalt. Detailed regional descriptions of the SRPA can be found in Holdren et al. 1997 and DOE-ID 1997.

Additional factors impacting groundwater flow are: (1) local recharge, (2) variations in hydraulic conductivity, (3) local pumping, and (4) possibly vertical hydraulic gradients. Groundwater directly beneath the proposed site is complex because the geology and water sources are complex; however, the general flow is predominantly to the south with a more southwest component nearer to the CFA. The local flow pattern likely results from production well pumping and from local recharge (i.e., BLR channel) that create the perched water observed in the vadose zone. The local hydraulic gradient is low, only 0.2 m/km (1.2 ft/mi) compared to the regional gradient of 0.8 m/km (4 ft/mi).

Groundwater beneath INTEC is approximately 137 m (450 ft) bls. Regional groundwater flow is south-southwest. The hydraulic conductivity of the SRPA near INTEC was estimated using the transmissivity values reported by Ackerman (1991) and the saturated thickness of the open interval of the

well. The estimation of hydraulic conductivity was based on the assumption that the wells fully penetrate the saturated thickness of the aquifer. Hydraulic conductivities range five orders of magnitude with a maximum of 3.0×10^{3} m/day (1.0×10^{4} ft/day) at well CPP-3 and a minimum of 3.0×10^{-2} m/day (1.0×10^{-1} ft/day) at Well USGS-114. The average hydraulic conductivity within the immediate vicinity of INTEC is $4.0 \times 10^{2} \pm 7.9 \times 10^{2}$ m/day ($1.3 \times 10^{3} \pm 2.6 \times 10^{3}$ ft/day). Using the average hydraulic conductivity—a hydraulic gradient of 1.2 m/km (6.3 ft/mi) (Cecil et al. 1991)—and an effective porosity of 10%, the calculated seepage velocity near the INTEC is approximately 3 m/day (10 ft/day). Groundwater flow velocities have also been estimated by observation of tritium concentration changes in wells downgradient of the INTEC injection well.

Hydraulic properties beneath the proposed site are not yet characterized. Hydraulic parameters measured at INTEC may be representative of the new location; however, site-specific data is required not only to confirm the site suitability, but also to narrow the uncertainty associated with previous data.

3.5 Meteorology and Climatology

Meteorological and climatological data that apply to INTEC and the surrounding INEEL region are collected and compiled from several meteorological stations operated by the National Oceanic and Atmospheric Administration field office in Idaho Falls, Idaho. Three stations are located on the INEEL at (1) CFA, (2) TAN, and (3) RWMC. No data are collected specifically for INTEC.

3.5.1 Precipitation

Although annual rainfall at the INEEL is light, and the region is classified as arid to semiarid (Clawson et al. 1989), natural recharge from precipitation contributes to the support of perched water bodies. The long-term average annual precipitation at the INEEL is 22.1 cm (8.7 in.). Monthly precipitation is usually highest in April, May, and June and lowest in July. If precipitation that falls in November through February falls as snow and remains on the ground until February, then an average 6.9 cm (2.7 in.) of water is available to infiltrate when evapotranspiration is low. Normal winter snowfall occurs from November through April, though occasional snowstorms occur in May, June, and October. Snowfall at the INEEL ranges from a low of about 17.3 cm (6.8 in.) per year to a high of about 151.6 cm (59.7 in.) per year, and the annual average is 70.1 cm (27.6 in.) (Clawson et al. 1989). In general, precipitation falling at INTEC during the winter months will infiltrate into the subsurface with minimal contribution from evapotranspiration. During the summer months, evapotranspiration is a more important contributor in the hydrogeologic cycle.

An average of two to three thunderstorms occur monthly from June through August (EG&G 1981). Thunderstorms often are accompanied by strong gusty winds that may produce local dust storms. Precipitation from thunderstorms at the INEEL is generally light. Occasionally, however, rain resulting from a single thunderstorm exceeds the average monthly total precipitation (Bowman et al. 1984).

Estimated net recharge from precipitation at INEEL ranges from 0.4 to 10.2 cm/year (0.2 to 4 in./year) (Schmalz and Polzer 1969, Miller et al. 1990, Cecil et al. 1992, Magnuson and McElroy 1993).

3.5.2 Temperature

The average summer daytime maximum temperature is 28°C (83°F), while the average winter daytime maximum temperature is -0.6°C (31°F). From meteorological records of temperature readings taken at CFA during a 38-year period from 1950 through 1988, extremes have varied from a low of -44°C (-47°F) in January to a high of 38°C (101°F) in July (Clawson et al. 1989).

3.5.3 Humidity

Data collected from 1956 through 1961 indicate that the average relative humidity at the INEEL ranges from a monthly minimum of 18% during the summer months to a monthly maximum of 55% in the winter. The relative humidity is directly related to diurnal temperature fluctuations. Relative humidity reaches a maximum just before sunrise (the time of lowest temperature) and a minimum in mid-afternoon (the time of maximum daily temperature) (Clawson et al. 1989).

The potential annual evaporation from saturated ground surface at the INEEL is approximately 109 cm (43 in.) with a range from 102 to 117 cm (40 to 46 in.) (Clawson et al. 1989). Eighty percent of this evaporation occurs between May and October. During the warmest month (July), the potential daily evaporation rate is approximately 0.63 cm/day (0.25 in./day). During the coldest months (December through February), evaporation is low and may be insignificant. Actual evaporation rates are much lower than potential rates because the ground surface is rarely saturated. Evapotranspiration by the sparse native vegetation of the Snake River Plain is estimated at between 15 to 23 cm/year (6 to 9 in./year), or 4 to 6 times less than the potential evapotranspiration. Periods when the greatest quantity of precipitation water is available for infiltration (late winter to spring) coincide with periods of relatively low evapotranspiration rates (EG&G 1981).

3.5.4 Wind

Wind patterns at the INEEL can be complex. The orientations of the surrounding mountain ranges and the ESRP play an important part in determining the wind regime. The INEEL is in the belt of prevailing westerly winds, which are channeled within the plain to produce a west-southwesterly or southwesterly wind approximately 40% of the time. The average midspring wind speed recorded at the CFA meteorological station at 6 m (20 ft) was 9.3 mph, while the average midwinter wind speed recorded at the same location was 5.1 mph (Irving 1993).

The INEEL is subject to severe weather episodes throughout the year. Thunderstorms with occasional tornadoes are observed mostly during the spring and summer. The tornado risk probability is about 7.8E-05 per year for the INEEL area (Bowman et al. 1984). Dust devils also are common in the region. Dust devils can entrain dust and pebbles and transport them over short distances. They usually occur on warm sunny days with little or no wind. The dust cloud may be several hundred yards in diameter and extend several hundred feet in the air (Clawson et al. 1989).